



Modelling of irradiance variations through atmosphere models

N. A. Krivova and S. K. Solanki

Max-Planck-Institut für Sonnensystemforschung, Max-Planck-Str. 2, 37191, Katlenburg-Lindau, Germany; e-mail: natalie@mps.mpg.de

Abstract. Regular space-based measurements of solar total and spectral irradiance reveal its variations on time scales from minutes to decades. About 90% of these variations are reproduced by recent models assuming that the evolution of the solar surface magnetic fields is their main cause. Circumstantial evidence suggests that variations on yet longer time scales, which are of special interest for climate studies, are also possible. Once good understanding of the directly observed variations has been gained, we can then attempt to extend the models back in time. Here a brief overview of our recent efforts to reconstruct solar total and spectral irradiance on time scales of days to centuries is given.

Key words. Sun: activity – Sun: faculae, plagues – Sun: irradiance – Sun: magnetic fields – solar-terrestrial relations – sunspots – Sun: UV radiation

1. Introduction

Solar total and spectral irradiance varies on all time scales on which it has been measured. These variations are of obvious interest for Sun-climate studies: any changes in the total solar irradiance (TSI) can affect the overall energy balance of the Earth's atmosphere, whereas variations in its spectral distribution have an important bearing on the chemistry of the Earth's upper atmosphere (Haigh, 1994, 1996, 2001; Larkin et al., 2000; Rind, 2002; Egorova et al., 2004; Rozanov et al., 2004). Unfortunately, the period over which direct measurements of the solar irradiance are available is too short to allow definite conclusions regarding the influence of the irradiance variations on climate. A sufficiently long reconstruction back to the pre-satellite period can

only be derived with the help of suitable models.

Construction of such models requires an understanding of the physical mechanisms of irradiance changes, including replicating their direct measurements. Solar irradiance variations can originate in the Sun's quiet photosphere or from the changing structure of the solar surface. The latter implies that the radiation coming from the quiet photosphere does not change. Rather, dark (sunspots) and bright (faculae and the network) features continuously appear and disappear on the solar surface and traverse the visible solar disc as the Sun rotates, thus modulating solar irradiance. Here only models of the second kind will be discussed. Recent progress in modelling observed variations of the solar total and spectral irradiance is summarised in Sects. 2 and 3, respect-

Send offprint requests to: N.A. Krivova

tively. Our efforts to extend the model back to the Maunder minimum are outlined in Sect. 4.

2. Solar cycle variations of the TSI

SATIRE (Spectral And Total Irradiance REconstructions, Solanki & Krivova, 2005; Solanki et al., 2005) is a set of irradiance models based on the assumption that all variations on time scales longer than approximately half a day are caused by the evolving surface distribution of the Sun's magnetic field. The surface magnetic features are divided into classes (atmospheric components), each described by a characteristic brightness spectrum. These spectra are calculated from the corresponding model atmospheres (Unruh et al., 1999). In the current version of SATIRE, the solar photosphere is represented by a 4-component model. Firstly, the solar model atmosphere of Kurucz (1991) in radiative equilibrium with an effective temperature of 5777K is used to calculate the intensity spectrum of the quiet photosphere (solar surface almost free of magnetic field). Next, sunspot umbral and penumbral fluxes are calculated from similar but cooler model atmospheres with effective temperatures of 4500 and 5400K, respectively (Unruh et al., 1999). Finally, the model employed for faculae and the network is an adaption of the model P of Fontenla et al. (1993) made by Unruh et al. (1999), who excluded the temperature inversion in the upper atmosphere and made further modifications in order to achieve better agreement with observations. All fluxes calculated in this way depend on the wavelength but are time-independent. A future alternative to using empirically derived model atmospheres is to employ the output of realistic 3-D numerical simulations of magnetoconvection such as those described by Vögler et al. (this issue), cf. Vögler et al. (2005).

Variations of the irradiance in time come from the second ingredient of SATIRE, the filling factors, which describe the fraction of the solar visible surface occupied by each photospheric component and evolve with time. They can be taken from observations or alternatively from flux transport simulations, such as those

of Schrijver et al. (2003) or Baumann et al. (2004). We use magnetograms and continuum images recorded at the Kitt Peak National Solar Observatory (KP/NSO, Livingston et al., 1976; Jones et al., 1992) and by the Michelson Doppler Interferometer (MDI, Scherrer et al., 1995) on SoHO.

Intensity images are employed to identify sunspots. Different brightness thresholds are used to separate umbrae (u) and penumbrae (p). Since sunspots are larger than the size of an individual MDI pixel ($2'' \times 2''$), a pixel which falls within a sunspot is assumed to be covered by it completely. In other words, the sunspot filling factor, $\alpha_{u,p}$, of such a pixel is 1. Alternatively, $\alpha_{u,p} = 0$, if a pixel is lying outside the sunspot.

All pixels identified as belonging to sunspots are excluded from the subsequent analysis of the magnetograms and all remaining magnetic signal above the noise level is assigned to faculae and the network, which are described by the same model atmosphere in the current version of SATIRE. Facular and network elements are typically smaller than an MDI pixel. So that the pixel may partly also cover the quiet solar surface. To describe this state of affairs a facular filling factor, α_f , is introduced, which denotes the fraction of the pixel covered by the facular or network component. The filling factor, α_f , grows linearly with the strength of the magnetic field until the saturation magnetic flux, Φ_{sat} , at which α_f reaches unity. Above this flux the pixel is assumed to be completely covered by faculae ($\alpha_f = 1$). Based only on the magnetograms we use, this saturation flux cannot be fixed precisely and is thus a free parameter of the model. It is fixed from a comparison with the observed total irradiance.

In this way, every individual pixel of a magnetogram is analysed, in order to find whether it lies within a sunspot or a facular region. Everything that does not belong to active regions and the network is counted to the quiet Sun: $\alpha_q = 1 - \alpha_u - \alpha_p - \alpha_f$. The brightness of each pixel, $F_{\text{px}}(\mu, \lambda, t)$, is then given by

$$F_{\text{px}}(\mu, \lambda, t) = \sum_{i=q,u,p,f} \alpha_i(t) F_i(\mu; \lambda),$$

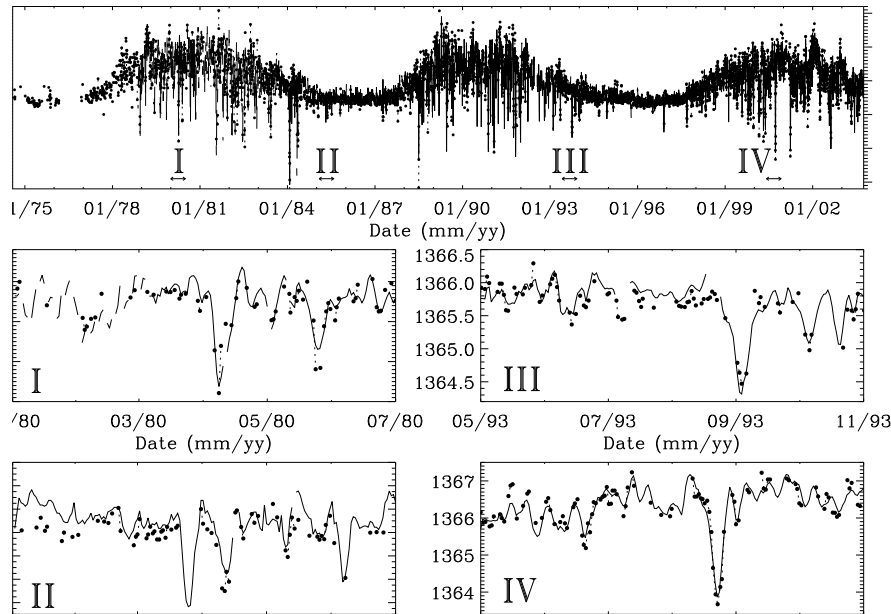


Fig. 1. Top panel: The reconstructed TSI (filled circles, connected by dotted curve when there are no data gaps) based on NSO/KP data between 1974 and 2003. The solid line represents the measured total solar irradiance (PMOD composite, Fröhlich, 2004) between 1978 and 2003. The bottom panels are enlargements of four shorter intervals at different activity levels from different cycles (from Wenzler et al., 2005b).

where $\mu = \cos(\theta)$ and θ is the heliocentric angle, λ is the wavelength, t time and $F_{q,u,p,f}$ are the brightnesses of the quiet Sun, umbrae, penumbrae and faculae (including the network), respectively. The sum over all pixels gives the solar irradiance at a given wavelength and an integral over all wavelengths the total solar irradiance.

We first employed the most homogeneous available data set, the one from the MDI, in order to reconstruct solar irradiance in cycle 23. With a single free parameter we reproduce very well both the short- (days to weeks) and long-term (years to the solar cycle) variations of the total irradiance. The correlation coefficient between the measured and modelled irradiances is 0.96 (Krivova et al., 2003).

Employment of the KP/NSO data allows an extension of the reconstruction back to 1974, i.e. to the time before the first satellite mea-

surements of solar irradiance. These data suffer from variable seeing and artifacts in some of the images (Wenzler et al., 2004, 2005a). More seriously, the data were not recorded by the same instrument over the whole period. The first, the 512-channel Diode Array Magnetograph (Livingston et al., 1976), was improved a few times and in 1992 replaced by the spectromagnetograph (Jones et al., 1992). There are still some problems with the cross-calibration of the two data sets and earlier data remain of a noticeably lower quality. For example, it is impossible to distinguish between umbrae and penumbrae in older images and only the entire spot areas can be determined. Therefore the average ratio of umbral to sunspot area was determined for the period after 1992 and assumed to be the same over the earlier period (Wenzler et al., 2005b). As expected, the resulting reconstructed ir-

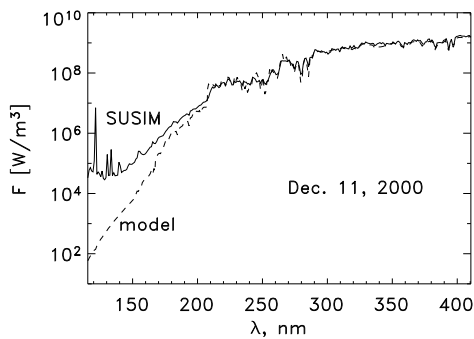


Fig. 2. Solar UV spectrum on December 11, 2000: observed (solid curve) by SUSIM on UARS (Brueckner et al., 1993; Floyd et al., 2003) and modelled (dashed) following Krivova et al. (2003).

radiance reproduces the TSI measurements (PMOD composite; see Fig. 1) somewhat less well than the MDI-based model. But, again, the agreement is quite good on both short and long time scales. The correlation coefficient is 0.91 for the whole period, 0.93 for the period after 1992 and no bias has been found between the three activity cycles (Wenzler et al., 2005b). This means that the evolution of the solar surface magnetic field indeed explains most, if not all, irradiance variations on the considered time scales, i.e. days to decades.

3. Solar spectral irradiance

As mentioned above, SATIRE provides both the total and spectral irradiance. Note that the free parameter, Φ_{sat} , is set from a comparison of the model with TSI and is kept the same when considering the spectral irradiance. Longwards of 400 nm, the model can be tested against VIRGO measurements in three spectral channels, red, green and blue centred at 862, 500 and 402 nm, respectively. The agreement on time scales of up to a few months is very good (Krivova et al., 2003) but on longer time scales the degradation trends in the data remain a problem for such a comparison.

The modelled spectra can also be compared with spectra recorded by, e.g., the SUSIM in-

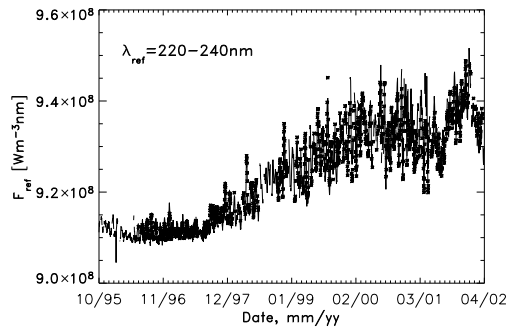


Fig. 3. The solar irradiance integrated over the wavelength range 220–240 nm as a function of time during 1996–2002. The solid line represents SUSIM measurements and asterisks the model by Krivova et al. (2003).

strument on UARS (Brueckner et al., 1993). Figure 2 shows the spectrum measured on a particular day by SUSIM (solid curve) and as obtained from our model (dashed). Above 300 nm the model is in good agreement with the measurements. Although stronger lines are not perfectly reproduced in the range between 200 and 300 nm, on average the model is relatively good here as well. At shorter wavelengths, the LTE approximation involved in calculations of the model atmospheres fails and the model spectrum lies systematically too low.

Krivova & Solanki (2005) have developed a technique allowing an empirical extension of the model down to 115 nm with the help of SUSIM data. As Fig. 3 shows, the model by Krivova et al. (2003) reproduces irradiance variations in the range 220–240 nm relatively well. On the other hand, SUSIM measurements can be used in order to work out empirical relations between the irradiance in this wavelength range and the irradiance at every other wavelength at which the data exist, i.e. between 115 and 410 nm. We employ daily level 3BS V21 data with spectral sampling of 1 nm (Floyd et al., 2003). The deduced relations are then used to calculate irradiance at every wavelength within this range from the reconstructed irradiance at 220–240 nm.

Figure 4 shows the relative irradiance variations between activity maximum (2 month

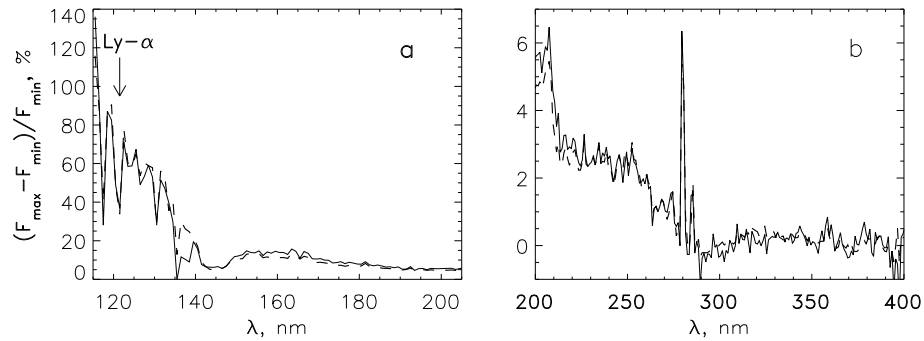


Fig. 4. Relative irradiance variations between the solar spectrum at activity maximum (2-month average, April–May 2000) and minimum (2-month average, October–November, 1996) at (a) 115–210 nm and (b) 200–420 nm. The solid line represents SUSIM measurements and the dashed line the model by Krivova & Solanki (2005).

average over April–May 2000) and minimum (October–November 1996). The solid line represents SUSIM measurements and the dashed line our reconstruction. The figure demonstrates the consistency between the empirical model and the SUSIM measurements.

Now, if the original and modified models are combined, they cover a broad wavelength range (115 nm – 160000 nm), which allows the contribution of different wavelength ranges to solar irradiance and to its variations to be estimated. At $\lambda \geq 300$ nm, the long-term uncertainty of SUSIM measurements is higher than the solar cycle variation. As a result, the relative difference between solar irradiance at activity maximum and minimum, as estimated from SUSIM data sometimes goes negative (see Fig. 4b), which is an artifact. Therefore the empirical model based on SUSIM data is used only at $\lambda < 290$ nm, whereas the original SATIRE model is employed at $\lambda \geq 290$ nm.

The calculated contribution of different wavelength ranges to solar irradiance and its 11-year cycle variation is shown in Fig. 5. The dashed line describes the distribution of the energy over the solar spectrum. Note the different size of bins: 50 nm in the UV, 100 nm in the visual and 2000 nm in the IR. The solid line shows the spectral distribution of the irradiance changes over the solar cycle. Although about 30% of solar energy comes from the long

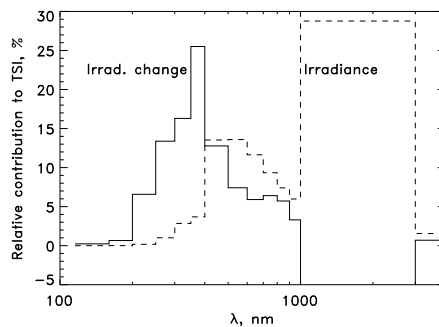


Fig. 5. The histograms of the spectral distribution of the solar energy (dashed) and of the solar cycle irradiance variations (solid). Note different size of bins (50 nm at $\lambda \leq 400$ nm, 100 nm at $400 \text{ nm} < \lambda \leq 1000$ nm and 2000 nm at longer λ).

wavelengths (> 1000 nm), their contribution to the irradiance variations is small: it is negative at 1000–3000 nm due to sunspots and is about 1–1.5% at yet longer λ . In contrast, the contribution of the UV irradiance variations is very high: the wavelength interval 300–400 nm accounts for about 40% of the TSI variations and about 60% of all TSI variations originate in the range between 200 nm and 400 nm. Of course, it will be particularly interesting to test

the spectral irradiance due to the SATIRE models using the SORCE (Woods et al., 2000) and SCIAMACHY (Skupin et al., 2005) spectral irradiance measurements.

4. Secular change in the solar irradiance

The success of our models in reproducing the directly observed irradiance variations suggests that given the distribution of the solar surface magnetic field, the irradiance can be calculated with significant precision. But how do we know the evolution of the solar magnetic field? This is relatively straightforward for its cyclic variation compared to a possible secular trend. A number of historical proxy records of solar magnetic activity, such as the Zurich or group sunspot number, sunspot areas, facular areas etc. exist, which can and have been employed in order to reconstruct irradiance variations back to the Maunder minimum (e.g., Foukal & Lean, 1990; Hoyt & Schatten, 1993; Zhang et al., 1994; Lean et al., 1995; Solanki & Fligge, 1998, 1999; Lockwood & Stamper, 1999; Fligge & Solanki, 2000; Foster, 2004). However, the magnitude of any secular change, which can be of even greater importance for Sun-climate studies remains controversial (for a discussion, see, e.g., Solanki & Krivova, 2005).

A simple physical mechanism for producing a secular trend of the magnetic field was proposed by Solanki et al. (2000, 2002). It is based on the overlap between activity cycles. Thus, the ephemeral regions start to erupt before the sunspot cycle begins and while the previous cycle is still running (Harvey, 1992). This overlap between activity cycles builds up a background magnetic flux, which is present on the solar surface even at activity minima (Harvey, 1994; Krivova & Solanki, 2004). The amount of this background flux depends on the strength of and the overlap between activity cycles. Since in particular the cycle strength varies significantly from one cycle to the next this leads to a secular variation of the background flux. More details about the model and the results are given by Solanki et al. (2002)

and in the review by Solanki & Schüssler (this issue).

The modelled total solar magnetic flux as well as its components (i.e. the flux emerging at the solar surface in active, Φ_{act} , and ephemeral, Φ_{eph} , regions and the open flux, Φ_{op}) can be used to reconstruct solar irradiance back to the Maunder minimum. In order to separate sunspot and facular contributions to Φ_{act} , we use the sunspot area, when available, or the sunspot number records. The sunspot area is a composite of the Greenwich data for the period between 1874 and 1976, Russian records (stations from the former USSR) between 1977 and 1986 and observations from Mt. Wilson later on (see Balmaceda et al., this issue, for more details). This record is extended back to 1700 by parameterization of the sunspot number record. The sum of the magnetic flux from the ephemeral regions and the open flux describes the evolution of the network, which is responsible for the secular change. Finally, in order to convert the magnetic fluxes into irradiance we use the same scheme as developed for the short-term models (Sect. 2).

This simple model reproduces the observed variations of TSI reasonably well, but not as well as the one presented in Sect. 2, where detailed maps of the magnetic flux distribution were used. The magnetic flux model we use is not able to replicate all details that are available in such maps. In particular, since the activity cycles of the ephemeral regions are assumed to be similar in shape to those of the sunspot cycles and are just stretched in time, the model describes their evolution only in a very general manner. This leads to some deviations between the model and observations in the shape of the TSI cycles. The amplitude of the irradiance changes is reproduced fairly well, however.

The reconstructed irradiance for the whole period back to 1700 is shown in Fig. 6. Under the constraint that the model must reproduce as well as possible the observed irradiance and magnetic flux time series, it predicts a secular increase in the irradiance of about 0.1%, i.e. comparable to the solar cycle variation observed during recent cycles. This is close to recent estimates by Foster (2004) and Wang et al.

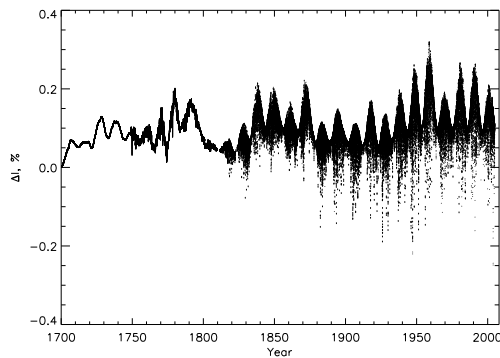


Fig. 6. The reconstructed total solar irradiance for the period 1700–2004 based on the model of Solanki et al. (2002) of the evolution of the Sun's magnetic flux.

(2005) but is lower than the previous appraisal of about 2–8 W/m² mainly (but not only) based on the comparison of the Ca II H and K emission of the Sun and other stars (White et al., 1992; Hoyt & Schatten, 1993; Zhang et al., 1994; Lean et al., 2001).

5. Summary

Models of the solar total irradiance have progressed to the stage where it is possible to reproduce the directly observed variations with high accuracy (Preminger et al., 2002; Krivova et al., 2003; Ermolli et al., 2003; Wenzler et al., 2004, 2005a). This suggests that a good understanding of the mechanisms of these variations has been reached.

One of such set of models, the SATIRE models, uses intensity spectra of the Sun's different photospheric magnetic components calculated from the corresponding model atmospheres and information (from models or observations) on the distribution of the magnetic flux on the solar surface, in order to figure out the total and spectral irradiance variations. The model works well for the total irradiance and in the spectral ranges longwards of about 200–300 nm where it has been tested (Unruh et al., 1999; Krivova et al., 2003). A recently developed empirical technique based on the observed SUSIM spectra allows an empirical

extension of the SATIRE models to shorter wavelengths (down to about 115 nm), which are of great interest to Sun-climate studies. Of course, a need for NLTE models remains (e.g., Fontenla, this issue; Haberreiter et al., 2005). The models still need to be tested in the IR. Such tests can and need to be done now using the new spectral data from SORCE (Harder et al., this issue) and SCIAMACHY (Skupin et al., 2005) launched in 2003.

On longer time scales, some sacrifice of the quality of the models is unavoidable due to the noticeable degradation of the amount and quality of the available proxies of solar magnetic activity. The challenge is a reconstruction of the general behaviour of the solar irradiance at earlier times, which is of crucial importance for evaluating the solar influence on the Earth's climate. Specifically, the magnitude of the secular change remains controversial. The first, stellar evidence for such a change (Baliunas & Jastrow, 1990; White et al., 1992) is now subjected to question, and its magnitude might have been overestimated (Foster, 2004; Wang et al., 2005). A simple physical model of the Sun's magnetic flux constructed by Solanki et al. (2000, 2002) put forward a physical explanation for such a change. An overlap between consecutive activity cycles (e.g. due to ephemeral regions) leads to the variable level of the background magnetic flux. A reconstruction of the solar total irradiance based on this model of the Sun's magnetic flux evolution yields for the secular change a value comparable to the recent solar cycle variation. However, further work is needed in this direction.

Acknowledgements. We thank T. Wenzler, L. Floyd and Y.C. Unruh for interesting and helpful discussions and L. Balmaceda for providing Fig. 6.

References

- Baliunas, S. & Jastrow, R. 1990, *Nature*, 348, 520
- Baumann, I., Schmitt, D., Schüssler, M., & Solanki, S. K. 2004, *A&A*, 426, 1075
- Brueckner, G. E., Edlow, K. L., Floyd, L. E. et al. 1993, *JGR*, 98, 10695
- Egorova, T., Rozanov, E., Manzini, E. et al. 2004, *GRL*, 31, 6119

- Ermolli, I., Berrilli, F., & Florio, A. 2003, *A&A*, 412, 857
- Fligge, M. & Solanki, S. K. 2000, *GRL*, 27, 2157
- Floyd, L. E., Cook, J. W., Herring, L. C., & Crane, P. C. 2003, *Adv. Sp. Res.*, 31, 2111
- Fontenla, J. M., Avrett, E. H., & Loeser, R. 1993, *ApJ*, 406, 319
- Foster, S. 2004, PhD thesis, University of Southampton, Faculty of Science, School of Physics and Astronomy
- Foukal, P. & Lean, J. 1990, *Science*, 247, 556
- Fröhlich, C. 2004, AGU Fall Meeting Abstracts, A301
- Haberreiter, M., Krivova, N. A., Schmutz, W., & Wenzler, T. 2005, *Adv. Sp. Res.*, 35, 365
- Haigh, J. D. 1994, *Nature*, 370, 544
- Haigh, J. D. 1996, *Science*, 272, 981
- Haigh, J. D. 2001, *Science*, 294, 2109
- Harvey, K. L. 1992, in ASP Conf. Ser. 27: The Solar Cycle, 335–367
- Harvey, K. L. 1994, in IAU Coll. 143: The Sun as a Variable Star: Solar and Stellar Irradiance Variations, ed. J. M. Pap, C. Fröhlich, H. S. Hudson, & S. K. Solanki (Cambridge: Cambridge Univ. Press), 217–225
- Hoyt, D. V. & Schatten, K. H. 1993, *JGR*, 98, 18895
- Jones, H. P., Duvall, T. L., Harvey, J. W., et al. 1992, *Sol. Phys.*, 139, 211
- Krivova, N. A. & Solanki, S. K. 2004, *A&A*, 417, 1125
- Krivova, N. A. & Solanki, S. K. 2005, *Adv. Sp. Res.*, 35, 361
- Krivova, N. A., Solanki, S. K., Fligge, M., & Unruh, Y. C. 2003, *A&A*, 399, L1
- Kurucz, R. L. 1991, in *Stellar Atmospheres - Beyond Classical Models*, ed. L. Crivellari, I. Hubeny, & D. G. Hummer (Dordrecht: Kluwer), 441–448
- Larkin, A., Haigh, J. D., & Djavidnia, S. 2000, *Sp. Sci. Rev.*, 94, 199
- Lean, J., Beer, J., & Bradley, R. 1995, *GRL*, 22, 3195
- Lean, J. L., White, O. R., Livingston, W. C., & Picone, J. M. 2001, *JGR*, 106, 10645
- Livingston, W. C., Harvey, J., Slaughter, C., & Trumbo, D. 1976, *Appl. Opt.*, 15, 40
- Lockwood, M. & Stamper, R. 1999, *GRL*, 26, 2461
- Preminger, D. G., Walton, S. R., & Chapman, G. A. 2002, *JGR*, 107, 1354, doi:10.1029/2001JA009169
- Rind, D. 2002, *Science*, 296, 673
- Rozanov, E. V., Schlesinger, M. E., Egorova, T. A., et al. 2004, *JGR (Atmospheres)*, 109, 1110; doi:10.1029/2003JD003796
- Scherrer, P. H., Bogart, R. S., Bush, R. I., et al. 1995, *Sol. Phys.*, 162, 129
- Schrijver, C. J., DeRosa, M. L., & Title, A. M. 2003, *ApJ*, 590, 493
- Skupin, J., Noël, S., Wuttke, M. W., et al. 2005, *Adv. Sp. Res.*, 35, 370
- Solanki, S. K. & Fligge, M. 1998, *GRL*, 25, 341
- Solanki, S. K. & Fligge, M. 1999, *GRL*, 26, 2465
- Solanki, S. K. & Krivova, N. A. 2005, *Sol. Phys.*, 224, 197
- Solanki, S. K., Krivova, N. A., & Wenzler, T. 2005, *Adv. Sp. Res.*, 35, 376
- Solanki, S. K., Schüssler, M., & Fligge, M. 2000, *Nature*, 408, 445
- Solanki, S. K., Schüssler, M., & Fligge, M. 2002, *A&A*, 383, 706
- Unruh, Y. C., Solanki, S. K., & Fligge, M. 1999, *A&A*, 345, 635
- Vögler, A., Shelyag, S., Schüssler, M., et al. 2005, *A&A*, 429, 335
- Wang, Y.-M., Lean, J. L., & Sheeley, N. R. 2005, *ApJ*, 625, 522
- Wenzler, T., Solanki, S. K., & Krivova, N. A. 2005a, *A&A*, 432, 1057
- Wenzler, T., Solanki, S. K., Krivova, N. A., & Fluri, D. M. 2004, *A&A*, 427, 1031
- Wenzler, T., Solanki, S. K., Krivova, N. A., & Fröhlich, C. 2005b, *A&A*, in preparation
- White, O. R., Skumanich, A., Lean, J. et al. 1992, *PASP*, 104, 1139
- Woods, T. N., Rottman, G. J., Harder, J. W., et al. 2000, in *Earth Observing Systems V*, SPIE Proceedings, ed. W. L. Barnes, Vol. 4135, 192
- Zhang, Q., Soon, W. H., Baliunas, S. L., et al. 1994, *ApJ Lett.*, 427, L111